Int. J. Solids Structures, 1967, Vol. 3, pp. 677 to 689. Pergamon Press Ltd. Printed in Great Britain

COLLAPSE OF A SIMPLY SUPPORTED CIRCULAR PLATE UNDER TWO UNIFORM LOADS

W. FLÜGGE

Standford University, Stanford, California

and

J. C. GERDEEN

Advanced Solid Mechanics Division, Battelle Memorial Institute, Columbus, Ohio

Abstract—Bending of a simply supported circular plate under two uniform normal loads of different magnitudes in the central region and outer annulus is considered. A rigid, perfectly plastic material is assumed which obeys the Tresca yield condition. Exact solutions are determined in terms of the radial and circumferential bending moments. A complete two-parameter collapse–load diagram is constructed which is piecewise regular. A variety of collapse mechanisms is exhibited for various ratios of the loads. In particular, a "two-way" deflection mode is found—the plate can deflect either "up" or "down" at a certain ratio of opposing loads. A new result of special significance is shown—portions of some stress trajectories lie within the rigid-domain bounded by the yield surface.

NOTATION

The notation used corresponds largely to that of Hodge [1]. An exception occurs where shell notation for the transverse shear has been preferred ([3], p. 313). Actual quantities are first defined and then dimensionless quantities are introduced. Rotational symmetry applies:

H	half thickness, length
R	radial coordinate, length
θ	angular coordinate
R_0	outside radius, length
K_R	curvature in radial direction, l/length
K_θ	curvature in circumferential direction, l/length
W	deflection normal to plate, length
M_R	radial bending moment, length-force/length
M_θ	circumferential bending moment, length-force/length
M_0	yield bending moment
Q	transverse shear stress resultant, force/length
P	transverse surface pressure, force/area
$\mathbf{Q}(m_r, m_\theta)$	generalized stress vector
$\mathbf{q}(\kappa_r, \kappa_\theta)$	generalized strain vector
$\mathbf{p}_c(p_1, p_2)$	collapse load vector

Dimensionless quantities:

$$h = \frac{H}{2R_0}, \qquad r = \frac{R}{R_0}, \qquad w = \frac{H}{2R_0^2}W$$
$$\kappa = \frac{H}{2}K, \qquad m = \frac{M}{M_0}, \qquad p = \frac{R_0^2}{6M_0}P, \qquad q = \frac{H}{2M_0}Q. \tag{1}$$

Deformation states are discussed here in terms of conventional curvature κ and deflection w. Actually, κ and w are incremental changes which occur at collapse. Those who prefer can substitute curvature rates $\dot{\kappa}$ and velocity $\dot{w}$.

INTRODUCTION

COLLAPSE of circular plates under combined loading has been considered by Hodge ([1], p. 42) and Drucker and Hopkins [2]. The former dealt with two uniform loadings as considered herein but only with positive loads, i.e. both acting in the same direction. The latter dealt with a concentrated load and a uniform load on an overhanging plate with the simple support as a special case. The latter analysis also pertained only to positive loads. It is the purpose of the present analysis to study the complex collapse behavior that can exist when the loads oppose one another.

DESCRIPTION OF THE PROBLEM

Exact solutions for the collapse loads and the incipient deflections are desired for the rotationally symmetric problem of a simply-supported circular plate loaded transversely by one uniform pressure, P_1, in a central region and by a second uniform pressure, P_2, in a concentric annular region. The positive senses of the loads and the dimensions of the plate are shown in Fig. 1.

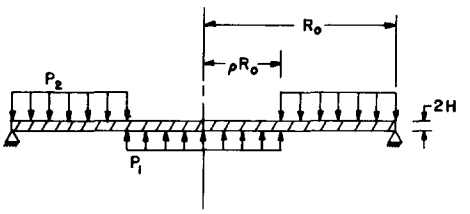

FIG. 1. Loading and dimensions of the circular plate.

The equilibrium equations and kinematic relations for rotationally symmetric bending of a circular plate take the following form in the dimensionless variables ([1], p. 40):

$$\left(\frac{rq}{h}\right)' + 6rp = 0$$

$$(rm_r)' - m_\theta = \frac{rq}{h} = -6\int_0^r sp(s)\,ds \qquad (2a\text{–}c)$$

$$\kappa_\theta = \frac{-w'}{r}, \qquad \kappa_r = -w'' \qquad (3a,b)$$

$$(\ )' \equiv \frac{d(\ )}{dr}.$$

For the problem of Fig. 1, the right-hand side of equilibrium equation (2c) is integrated for the two regions, $0 \leqq r \leqq \rho$ and $\rho \leqq r \leqq 1$, where p_1 and p_2 are dimensionless forms of P_1 and P_2, respectively. After integration and combination with equation (2b), two equilibrium equations result for the two regions:

$$(rm_r)' - m_\theta = 3p_1 r^2, \qquad 0 \leqq r \leqq \rho \qquad (4)$$

$$(rm_r)' - m_\theta = 3(p_1 + p_2)\rho^2 - 3p_2 r^2, \qquad \rho \leqq r \leqq 1. \qquad (5)$$

The external energy dissipation rate is

$$D = \int_0^{R_0} PW \,.\, 2\pi R \,\mathrm{d}R.$$

This is put into a dimensionless form d as follows

$$d = \frac{H}{4\pi M_0 R_0^2} \,.\, D = 6\int_0^1 pwr \,\mathrm{d}r.$$

For the present problem d becomes

$$d = -6p_1\int_0^{\rho} wr \,\mathrm{d}r + 6p_2\int_{\rho}^1 wr \,\mathrm{d}r. \tag{6}$$

The plate material is assumed to be rigid-perfectly plastic and to obey the Tresca yield condition. This yield condition in the two-dimensional space of the generalized stresses m_r and m_θ is shown in Fig. 2. Stress points $\mathbf{Q}(m_r, m_\theta)$ inside the yield surface are less than yield and correspond to rigid body motions, those on the surface correspond to yield and possible nonzero strain, and those outside the surface are forbidden for a perfectly plastic material. Thus, a stress point $\mathbf{Q}(m_r, m_\theta)$ must obey the inequalities

$$\begin{aligned} &m_r \leqq 1, \qquad -m_r \leqq 1, \qquad m_\theta \leqq 1, \qquad -m_\theta \leqq 1, \\ &m_r - m_\theta \leqq 1, \qquad -m_r + m_\theta \leqq 1. \end{aligned} \tag{7a–f}$$

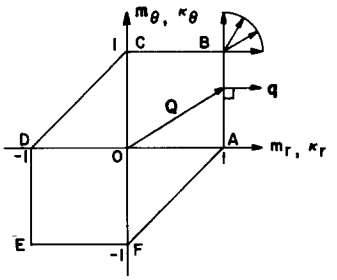

FIG. 2. Tresca yield condition.

The consecutive laws for a perfectly-plastic material have been developed by Drucker [4,5] based on the "plastic potential flow law" of von Mises [6] ([1], pp. 9–10). For a stress point $\mathbf{Q}(m_r, m_\theta)$ on a yield curve (e.g. $m_\theta = 1$), the resultant strain-rate vector $\mathbf{q}(\kappa_r, \kappa_\theta)$ originates at this point and is parallel to the outward-normal to the curve at that point. Thus, the following equations for curvature and deflection [from equations (3a,b)] apply for the six sides of the yield condition of Fig. 2:

on AB: $$\kappa_\theta/\kappa_r = 0, \qquad \kappa_r \geqq 0; \qquad w = A_1 \tag{8a}$$

on BC: $$\kappa_r/\kappa_\theta = 0, \qquad \kappa_\theta \geqq 0; \qquad w = A_2 r + B_2 \tag{8b}$$

on CD: $$\kappa_\theta/\kappa_r = -1, \qquad \kappa_\theta \geqq 0, \qquad \kappa_r \leqq 0; \qquad w = A_3 \log r + B_3 \tag{8c}$$

on DE: $$\kappa_\theta/\kappa_r = 0, \qquad \kappa_r \leqq 0; \qquad w = A_4 \tag{8d}$$

on EF: $$\kappa_r/\kappa_\theta = 0, \qquad \kappa_\theta \leqq 0; \qquad w = A_5 r + B_5 \tag{8e}$$

on FA: $$\kappa_r/\kappa_\theta = -1, \qquad \kappa_r \geqq 0, \qquad \kappa_\theta \leqq 0; \qquad w = A_6 \log r + B_6. \tag{8f}$$

Inside the hexagon ABCDEF the curvatures and deflections are:

$$\kappa_r = \kappa_\theta = 0, \qquad w = A_7. \tag{8g}$$

The A_i and B_i are arbitrary constants.

The boundary conditions for the circular plate of Fig. 1 are

$$m_r = 0, \qquad w = 0 \quad \text{at} \quad r = 1. \tag{9a,b}$$

Non-uniqueness of the r and θ directions at the center of the plate leads to the following condition:

$$m_r = m_\theta, \quad \text{at} \quad r = 0. \tag{10}$$

Also the deflection at the center is defined as

$$w \equiv w_0, \quad \text{at} \quad r = 0. \tag{11}$$

Other conditions are that w, m_r, and q must be continuous.

It is desired to find a complete collapse-load curve; i.e. a plot of p_1 vs. p_2 at collapse. Since the yield surface is convex it follows that the collapse-load curve must also be convex ([1], pp. 19–20). Therefore, convexity of the collapse-load curve can be used as a check on solutions. Since the Tresca yield surface is piecewise regular, and since different collapse behavior is likely for different load ratios p_1/p_2, it is expected that the collapse-load surface is also piecewise regular.

METHOD OF ANALYSIS

The Upper and Lower Bounds of Limit Analysis are employed. If a load $\mathbf{p}(p_1, p_2)$ can be shown to be both an upper bound to the collapse load $\mathbf{p}_c$; i.e., $|\mathbf{p}| \geqq |\mathbf{p}_c|$ and a lower bound, $|\mathbf{p}| \leqq |\mathbf{p}_c|$ then it is necessary that $\mathbf{p}$ is an exact solution; i.e., $\mathbf{p} = \mathbf{p}_c$. This is the method used here.

An upper bound is defined in terms of a kinematically admissible deflection solution: w is a solution that satisfies one or more of equations (8) and boundary condition (9b), w is continuous, all stress points $\mathbf{Q}(m_r, m_\theta)$ correspond to strain vectors $\mathbf{q}(\kappa_r, \kappa_\theta)$ associated with w through equations (8a–g), and positive work is done; i.e., $d > 0$. A lower bound is defined in terms of a statically admissible stress solution: m_r and m_θ are solutions of equilibrium equations (4) and (5), that also satisfy condition (10) and inequalities (7a–f), m_r satisfies boundary condition (9a), and m_r and q are continuous.

Solutions

The analysis is begun for the values of p_1 and p_2 considered by Hodge ([1], pp. 42–43); i.e., $p_1 < 0$, $p_2 > 0$, and the deflection everywhere positive and conical. This solution is called "Collapse Mode I".

Collapse Mode I. The stress trajectory of **Q** and the deflection mode are shown in Fig. 3(a). The solution is:

$$\begin{aligned} m_\theta &= 1 && , \quad 0 \leqq r \leqq 1 \\ m_r &= 1+p_1 r^2 && , \quad 0 \leqq r \leqq \rho \\ m_r &= (1-p_2 r^2)+(p_2+p_1)(3-2\rho/r)\rho^2, && \quad \rho \leqq r \leqq 1 \end{aligned} \tag{12a–c}$$

$$\begin{aligned} m_r' &= 2p_1 r && , \quad 0 \leqq r \leqq \rho \\ m_r' &= -2p_2 r+2(p_2+p_1)\rho^3/r^2 && , \quad \rho \leqq r \leqq 1 \end{aligned} \tag{13a,b}$$

$$w = w_0(1-r) \quad , \quad 0 \leqq r \leqq 1. \tag{14}$$

The moment solution (12a–c) satisfies the condition $m_r(0) = m_\theta(0)$ and is continuous at $r = \rho$.

The boundary condition (9a) substituted into equation (12c) gives a linear relationship between p_1 and p_2 for a fixed value of ρ:

$$-(3-2\rho)\rho^2 p_1+(1-p)^2(1+2\rho)p_2 = 1. \tag{15}$$

Equation (15) represents the exact collapse load if m_r satisfies condition (7a). For $r < \rho$, equation (12b) requires that

$$p_1 \leqq 0, \tag{16a}$$

and for $r > \rho$ it is necessary that $m_r' < 0$, which leads to

$$-p_2(1-\rho^3)+p_1\rho^3 \leqq 0, \tag{16b}$$

since for $p_2 > 0$ the maximum of m_r' occurs at $r = 1$. Equality in either (16a) or (16b) enables determination of limit values on p_1 and p_2 from solution (15). These are, respectively,

$$p_1 = 0, \qquad p_2 = \frac{1}{(1-\rho^2)(1+2\rho)}$$

and (17a,b)

$$p_1 = -\frac{1+\rho+\rho^2}{3\rho^2}, \qquad p_2 = -\frac{\rho}{3(1-\rho)}.$$

At the limit (17b), p_2 is no longer positive, but it may be verified that even for this load the inequality (16b) still assures $m_r \leq 1$ everywhere. It is evident for the first load point (17a) that positive work is done. For the second point (17b), substitution of p_1 and p_2 and w from (14) into (6) gives $d = w_0$. Thus, d is positive for positive w_0 and, therefore, the collapse load curve (15) is exact between the limits (17a, b).

At the limit point (17a) for which $p_1 = 0$, the state of stress for the entire region $0 \leqq r \leqq \rho$ corresponds to the one point B of the yield condition, Fig. 3(a) and Fig. 2. The deflection solution for this region is, therefore, not unique, because all strain vectors **q** of a 90°-fan are permitted; i.e., any deflection with positive κ_r and κ_θ is allowed. This lack of uniqueness at $p_1 = 0$ is indicated by the dashed lines in Fig. 3(a).

Collapse Mode II. For this solution the stress trajectory lies partly on side AB and partly on side BC of the yield limit as shown in Fig. 3(b). The deformation state consists of a

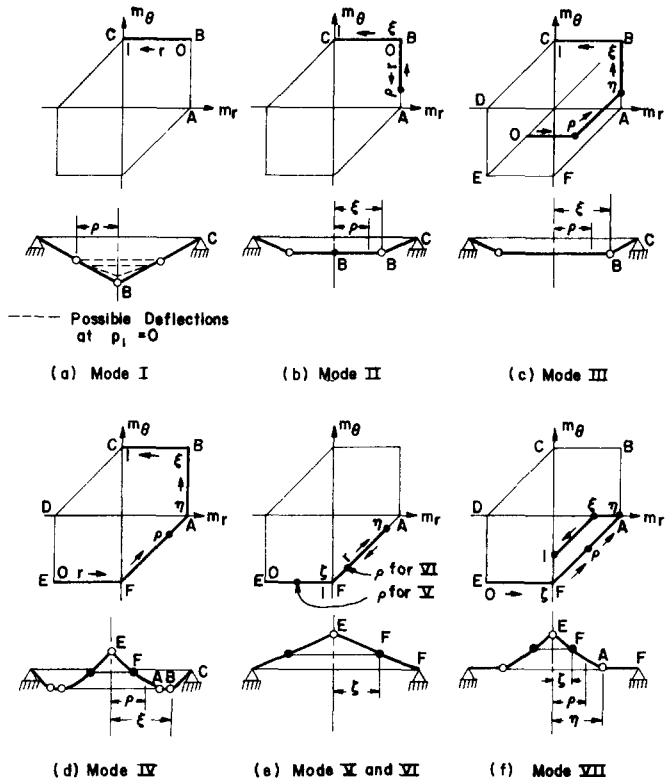

FIG. 3. Stress trajectories and incipient deflections for the collapse modes.

rigid-body translation in the central region. The results are:

$$m_r = 1, \qquad m_\theta = 1 - 3p_1 r^2,$$
$$m_\theta' = -6p_1 r \qquad , \qquad 0 \leqq r \leqq \rho \tag{18a–c}$$

$$m_r = 1, \qquad m_\theta = 1 + 3p_2 r^2 - 3(p_1 + p_2)\rho^2,$$
$$m_\theta' = 6p_2 r \qquad , \qquad \rho \leqq r \leqq \xi \tag{19a–c}$$

$$m_\theta = 1,$$
$$m_r = [3(p_1 + p_2)\rho^2 + 1](1 - 1/r) - p_2(r^2 - 1/r), \qquad \xi \leqq r \leqq 1. \tag{20a, b}$$

These moment-equations include the conditions $m_r(0) = m_\theta(0)$, $m_r(1) = 0$, and the condition of continuity of m_r at $r = \rho$. The conditions $m_\theta(\xi) = 1$ and $m_r(\xi) = 1$ substituted into equations (19b) and (20b) give, respectively:

$$(\xi^2 - \rho^2)p_2 - \rho^2 p_1 = 0$$
$$[(1 - \xi^3) - 3\rho^2(1 - \xi)]p_2 - 3\rho(1 - \xi)p_1 = 1. \tag{21a, b}$$

Equations (21a, b) constitute a nonlinear relation between p_1 and p_2 in terms of the radius parameter ξ.

For $0 \leqq r \leqq \rho$, the restrictions $m_\theta(\rho) \geqq 0$ and $m'_\theta \leqq 0$, imposed on solutions (18b, c), imply two inequalities for p_1:

$$p_1 \leqq \frac{1}{3\rho^2}, \qquad p_1 \geqq 0. \tag{22a, b}$$

The restriction $m'_\theta \geqq 0$ in solution (19c) gives:

$$p_2 \geqq 0. \tag{22c}$$

Equality in either (22a) or (22b) gives the following limits for Mode II from equations (21a, b):

$$p_1 = \frac{1}{3\rho^2}, \qquad p_2 = \frac{1}{3(\xi_2^2 - \rho^2)}, \qquad \text{where } \xi_2 > \rho, \tag{23a}$$

$$p_1 = 0, \qquad p_2 = \frac{1}{(1-\rho)^2(1+2\rho)}, \qquad \xi_1 = \rho \tag{23b}$$

and where

$$2\xi_2^3 - 6\xi_2^2 + 3\rho^2 + 1 = 0.$$

It can be shown that positive work is done for Mode II.

Collapse Mode III. Examination of Mode II in Fig. 3(b) suggests that the rigid body translation in the central region and the condition (10) can also be satisfied by another Mode III shown in Fig. 3(c). At a point η on side AB, the stress trajectory for $r \leqq \eta$ is permitted to lie in the rigid domain bounded by the yield surface ([7], pp. 27–28). For $0 \leqq r \leqq \eta$ the stress distribution is not unique. Any arbitrary solution to the equilibrium equations (4) and (5) which also satisfies inequalities (7a–f) and equation (10) is acceptable. The arbitrariness is due to the lack of a constitutive law in the rigid region $0 \leqq r \leqq \eta$. This shows the difference between a rigid-plastic material and an elastic-plastic material.

For this rigid-plastic solution the plastic part yet determines a collapse-load curve. For $\eta \leqq r \leqq \xi$, equations (19a–c) and inequality (22c) for side AB are valid. The conditions $m_\theta(\xi) = 1$ and $m_\theta(\eta) = m_1$ give

$$\begin{aligned} (\xi^2 - \rho^2)p_2 - \rho^2 p_1 &= 0 \\ 1 + 3p_2(\eta^2 - \rho^2) - 3p_1\rho^2 &= m_1, \end{aligned} \tag{24a, b}$$

where $0 \leqq m_1 \leqq 1$. For $\xi \leqq r \leqq 1$, equations (20a, b) and (21b) hold for side BC. Equations (24a) and (21b) enable a collapse-load curve to be plotted for Mode III for various values of the radius ξ. Since equation (24a) is identical to (21a), the collapse-load curve for Mode III is found to be a smooth continuation of the curve for Mode II.

It is easily shown that positive work is done for the p_1 and p_2 values for Mode III, and for kinematically admissible deflection values satisfying the solution equations (8a, b, g) and (11). In order to prove that equations (24a) and (21b) constitute an exact solution for p_1 and p_2, there yet remains to show that a statically admissible stress state exists for the rigid region $0 \leqq r \leqq \eta$. As an example, the stress trajectory in Fig. 3(c) is a statically admissible solution. For this trajectory the moment solution is

$$m_\theta = -m_2, \qquad m_r = -m_2 + p_1 r^2, \qquad \text{for} \quad 0 \leqq r \leqq \rho \tag{25a, b}$$

and

$$m_r - m_\theta = m_3, \qquad m_r = [-m_3 + 3(p_1+p_2)\rho^2]\log r/\eta - \frac{3}{2}p_2(r^2-\eta^2)+1, \qquad \text{for} \quad \rho \leqq r \leqq \eta, \tag{25c, d}$$

where $0 < m_2 < 1$ and $0 < m_3 < 1$. This solution has $m_r' > 0$, $m_r(0) = m_\theta(0)$, and $m_r(\eta) = 1$, as required. Continuity of m_r at $r = \rho$ gives one equation between the parameters m_1 and m_2. Thus, arbitrariness exists in the solution as indicated earlier.

Equation (24b) is one equation between m_1 and η which for $0 \leqq m_1 \leqq 1$ and $p_2 > 0$ implies $\rho \leqq \eta \leqq \xi$. The non-uniqueness in η means that the width of the plastic zone $\eta \leqq r \leqq \xi$ is not unique. Thus, in Mode III non-uniqueness is exhibited in two ways: the stresses in the rigid region $0 \leqq r \leqq \eta$ are not unique, and the width of the plastic region $\eta \leqq r \leqq \xi$ is not unique.

Collapse Mode IV. The stress trajectory of Collapse Mode III for $0 \leqq r \leqq \eta$ in Fig. 3(c), suggests that the stress trajectory of a new mode, IV, may lie on sides EF and FA for $0 \leqq r \leqq \eta$. This is the case as shown in Fig. 3(d). However, when this analysis is carried out it is found that this collapse mode is valid at only one point in the p_1, p_2 plane. This point is also a point for Mode III for which $m_1 = 0$ in equation (24b).

The detailed solution for Mode IV is not presented, since it exists for only one point and because the point (p_1, p_2) can also be found from solutions for Mode III and another Mode VII which is considered later.

For the deflection shown in Fig. 3(d), open circles indicate strong discontinuities, "yield hinges" (discontinuity in w'), and solid circles indicate weak discontinuities (continuity in w').

Collapse Mode V. In the analysis conducted so far, adjoining collapse modes have been found by first finding a side or sides of the Tresca hexagon common to both modes. However, this method becomes increasingly difficult to employ as the collapse modes have become more complex. Instead of seeking another mode adjoining the complex mode IV, it is more efficient to seek a connection to the simple mode, I. Mode I, Fig. 3(a) was originally found for $p_1 \leqq 0$. Mode I, reflected about the origin is also valid for $p_1 \geqq 0$ and has then side EF of the yield surface (Fig. 2) valid throughout the plate. Collapse Mode V is now considered for which yielding is defined partly by side FA in addition to side EF as shown in Fig. 3(e). The solution is as follows:

$$m_\theta = -1, \qquad m_r = -1 + p_1 r^2, \qquad m_r' = 2p_1 r, \qquad 0 \leqq r \leqq \rho \tag{26a–c}$$

$$\begin{aligned} &m_\theta = -1, \qquad m_r = [3(p_1+p_2)\rho^2 - 1](1-\zeta/r) - p_2(r^2-\zeta^3/r), \\ &m_r' = [3(p_1+p_2)\rho^2 - 1]\zeta/r^2 - p_2(2r+\zeta^3/r^2), \qquad \rho \leqq r \leqq \zeta \end{aligned} \tag{27a–c}$$

$$\begin{aligned} &m_\theta = m_r - 1, \qquad m_r = [3(p_1+p_2)\rho^2 - 1]\log r - \frac{3}{2}p_2(r^2-1), \\ &m_r' = [3(p_1+p_2)\rho^2 - 1]1/r - 3p_2 r, \qquad \zeta \leqq r \leqq 1. \end{aligned} \tag{28a–c}$$

This solution satisfies the conditions $m_r(0) = m_\theta(0)$, $m_r(\zeta) = 0$, and $m_r(1) = 0$. On side EF, the conditions $m_r(\rho) \leqq 0$ and $m_r'(\rho) \geqq 0$ require from equations (26a, c), that

$$p_1 \leqq \frac{1}{\rho^2} \qquad \text{and} \qquad p_1 \geqq 0. \tag{29a, b}$$

The conditions $m_r'(\zeta) \geqq 0$, $m_r'(\eta) = 0$, $m_r'(1) \leqq 0$, $m_r(\zeta) = 0$, and $m_r(\eta) \leqq 1$, substituted into equations (27c), (28c), (28c), (28b), and (28b), respectively, give:

$$\begin{aligned} 3(p_1+p_2)\rho^2 - 1 - 3p_2\zeta^2 &\geqq 0, \\ 3(p_1+p_2)\rho^2 - 1 - 3p_2\eta^2 &= 0, \\ 3(p_1+p_2)\rho^2 - 1 - 3p_2 &\leqq 0, \\ [3(p_1+p_2)\rho^2 - 1]\log\zeta - \frac{3}{2}p_2(\zeta^2-1) &= 0, \\ [3(p_1+p_2)\rho^2 - 1]\log\eta - \frac{3}{2}p_2(\eta^2-1) &\leqq 1. \end{aligned} \tag{30a–e}$$

Also, continuity of m_r at $r = \rho$ requires that equations (26b) and (27b) are equal:

$$-1 + p_1\rho^2 = [3(p_1+p_2)\rho^2 - 1][1 - \zeta/\rho] - p_2(\rho^2 - \zeta^3/\rho). \tag{30f}$$

The three equations (30b, d, f) in four unknowns p_1, p_2, ζ, and η define a collapse-load curve. The solution is exact if it can be shown that it is kinematically admissible and dissipates positive energy. The deflection solutions (8e) and (8f) which satisfy the conditions $w(1) = 0$, $w(0) = -w_0$, and $w(\xi)$ and $w'(\xi)$ continuous, are

$$\begin{aligned} w &= \frac{(r - \zeta + \zeta\log\zeta)}{\zeta(1-\log\zeta)}w_0, \qquad 0 \leqq r \leqq \zeta \\ w &= \frac{\log r}{1-\log\zeta}w_0 \qquad , \qquad \zeta \leqq r \leqq 1. \end{aligned} \tag{31a, b}$$

[Continuity of $w'(\zeta)$ is required because a strong discontinuity in the strain-rate vector $\mathbf{q}$ cannot be permitted at Point F ([1], p. 12).]

For $\eta = \zeta = 1$, equation (30b) implies equality in (30a) and (30c) and Mode V intersects Mode I. For $\zeta = \rho$, equation (30f) requires $p_1 = 1/\rho^2$, and (29a) becomes an equality. Equation (30d) then determines p_2. Thus, at the other limit point to Mode V, p_1 and p_2 are

$$p_1 = \frac{1}{\rho^2}, \qquad p_2 = \frac{-2\log\rho}{3[\rho^2\log\rho + 1/2(1-\rho^2)]}. \tag{32a, b}$$

It can be verified that positive energy is dissipated by substitution of (32a, b) and (31a, b) into (6).

Collapse Mode VI. A new collapse mode, VI, intersecting V at the point (32a, b) is easily found, which is based on the same sides of the yield condition. The difference is that $r = \rho$ now falls on side FA rather than on EF as indicated in Fig. 3(e). It follows, therefore, that the deflection solution (31a, b) is again valid, and that the stress solution is:

$$m_\theta = -1, \qquad m_r = -1 + p_1 r^2, \qquad m_r' = 2p_1 r, \qquad 0 \leqq r \leqq \zeta \tag{33a–c}$$

$$\begin{aligned} m_\theta &= m_r - 1, \qquad m_r = \frac{3}{2}p_1(r^2 - \zeta^2) - \log(r/\zeta), \\ m_r' &= 3p_1 r - \frac{1}{r}, \qquad \zeta \leqq r \leqq \rho \end{aligned} \tag{34a–c}$$

$$m_\theta = m_r - 1, \qquad m_r = [3(p_1+p_2)\rho^2 - 1]\log r - \frac{3}{2}p_2(r^2-1),$$
$$m_r' = [3(p_1+p_2)\rho^2 - 1]\frac{1}{r} - 3p_2 r, \qquad \rho \leqq r \leqq 1. \tag{35a–c}$$

This solution satisfies the conditions $m_r(0) = m_\theta(0)$, $m_r(\zeta) = 0$, and $m_r(1) = 0$ if

$$p_1 = \frac{1}{\zeta^2}. \tag{36}$$

For $\rho \leqq r \leqq 1$, the conditions $m_r(\eta) \leqq 1$ and $m_r'(\eta) = 0$, substituted into (35b, c), respectively, give

$$[3(p_1+p_2)\rho^2 - 1]\log\eta - \frac{3}{2}p_2(\eta^2-1) \leqq 1,$$
$$3(p_1+p_2)\rho^2 - 1 - 3p_2\eta^2 = 0. \tag{37a, b}$$

Continuity of m_r at $r = \rho$ in equations (34b) and (35b) requires:

$$\frac{3}{2}p_1(\rho^2-\zeta^2) - \log(\rho/\zeta) = [3(p_1+p_2)\rho^2 - 1]\log\rho - \frac{3}{2}p_2(\rho^2-1). \tag{38}$$

Equations (36), (37b), and (38) in the four unknowns, p_1, p_2, ζ, and η determine a collapse-load curve. As already indicated, $\zeta = \rho, p_1 = \frac{1}{\rho^2}$ is the point of intersection with Mode V [p_2 given by (32b)]. The other limit point to Mode VI occurs when (37a) becomes an equality. It can be found that positive energy is dissipated by substitution of p_1 and p_2 values and the deflection solutions (31a, b) into equation (6).

Collapse Mode VII. At the limit point $r = \eta$ of Mode VI corresponding to the vertex A, the stress trajectory can also enter within the yield surface ([7], pp. 27–28). Thus, the stress trajectory shown in Fig. 3(f) is considered for Mode VII. A rigid-body deflection, $w = 0$, is the solution for $\eta \leqq r \leqq 1$.

For $0 \leqq r \leqq \eta$, the yield conditions for sides EF and FA define yielding as before in Mode VI. For $\eta \leqq r \leqq 1$ the plate is rigid and **Q** traces a trajectory inside FA. As in Mode III, that part of the stress-trajectory within the yield surface is not unique.

Because of the similarity with Mode VI, equations (33a–c), (34a–c), (36), and (37b) also hold for this mode, VII. Equations (35a, c) also hold, but for $\rho \leqq r \leqq \eta$. Equation (35b) must be replaced by

$$m_r = [3(p_1+p_2)\rho^2 - 1]\log(r/\eta) - \frac{3}{2}p_2(r^2-\eta^2) + 1 \tag{39}$$

in order to satisfy the condition $m_r(\eta) = 1$. Continuity of m_r at $r = \rho$ now gives:

$$\frac{3}{2}p_1(\rho^2-\zeta^2) - \log(\rho/\zeta) = [3(p_1+p_2)\rho^2 - 1]\log(\rho/\eta) - \frac{3}{2}p_2(\rho^2-\eta^2) + 1. \tag{40}$$

For $\eta \leqq r \leqq 1$, any statically admissible stress solution may be permitted which satisfies the continuity conditions and boundary conditions. The trajectory shown in

Fig. 3(f) is an example. It corresponds to the following moment solution:

$$m_\theta = 0,$$

$$m_r = 3(p_1+p_2)\rho^2\left(1-\frac{\eta}{r}\right)-p_2\left(r^2-\frac{\eta^3}{r}\right)+\frac{\eta}{r}, \qquad \text{for} \quad \eta \leqq r \leqq \xi,$$

and

$$m_\theta = m_r - m,$$

$$m_r = [-m+3(p_1+p_2)\rho^2]\log r-\frac{3}{2}p_2(r^2-1), \qquad \text{for} \quad \xi \leqq r \leqq 1,$$

where $0 < m \leqq 1$. This solution satisfies the continuity condition at $r = \eta$ and the boundary condition $m_r = 0$ at $r = 1$. Also $m_r' < 0$ for $\eta \leqq r \leqq \xi$ as can be verified with use of equation (37b). Continuity of m_r at $r = \xi$ gives one equation between the unknowns m and ξ. Thus the solution is arbitrary to this degree. It is found that m or ξ can be chosen to provide $m_r' < 0$ for $\xi \leqq r \leqq 1$.

Although there remains some arbitrariness in the stress solution for $\eta \leqq r \leqq 1$, a collapse-load curve for Mode VII can be plotted using only equations (36), (37b), and (40). This is an exact collapse-load curve since it is also kinematically admissible; $d > 0$ as can be checked. The complete collapse-load diagram shown in Fig. 4 is now finished.

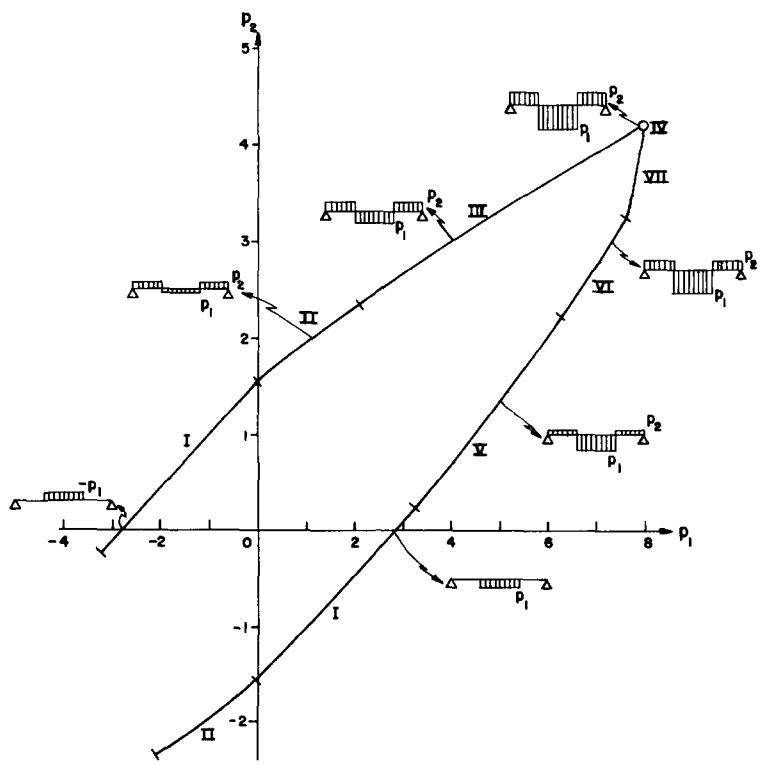

FIG. 4. Collapse-load diagram for a circular plate, $\rho = 0{\cdot}4$.

The point of intersection of Modes VII and III, where also Mode IV is valid, is an interesting point. At this point the deflection solution is not unique. There is a changeover from positive deflection to negative deflection and a transition in appearance of the deflected shape. The deflection profiles for these three modes are shown together in Fig. 5.

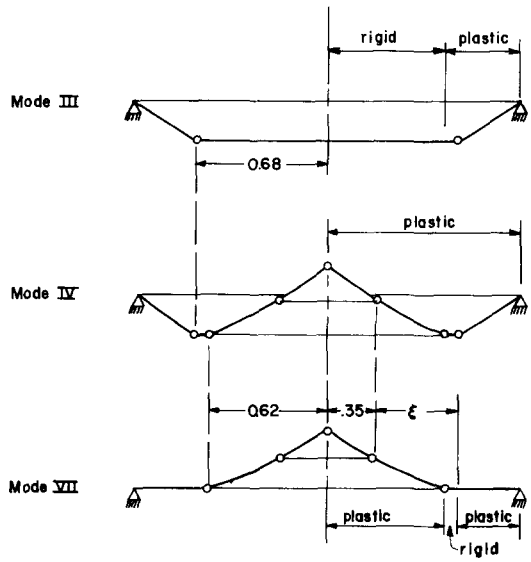

FIG. 5. Point of transition from Mode III to Mode IV to Mode VII, $p_1 = 7{\cdot}98$, $p_2 = 4{\cdot}20$, $\rho = 0{\cdot}4$.

The radii, $r = 0{\cdot}68$ and $r = 0{\cdot}62$ to the yield-hinge circles (strong discontinuities) are the same for Modes III and IV, and for Modes IV and VII, respectively.

CONCLUSIONS

A plate or shell of rigid-perfectly plastic material usually collapses at a definite load and in a specific shape for a loading defined by a single parameter. Under multiple loading, however, there is an interplay of load parameters which characterizes several different collapse mechanisms. A simply supported circular plate loaded by two uniform pressures, a two-load parameter problem, is an example. In this case, seven independent collapse modes are possible each for a different range of the load parameters. In five of the modes, the whole plate yields according to one or more sides of the Tresca yield condition. In the other two modes, only part of the plate is wholly plastic, and other parts are rigid with stress trajectories within the yield surface. The partially rigid, partially plastic collapse occurs for opposing loads. Also, when the loads oppose one another, the deflection solution may not be unique, but yet has to be a linear combination of a finite number of possibilities.

REFERENCES

[1] P. G. HODGE, *Limit Analysis of Rotationally Symmetric Plates and Shells*. Prentice-Hall (1963).
[2] D. DRUCKER and H. HOPKINS, Combined concentrated and distributed load on ideally-plastic circular plates. *Proc. 2nd U.S. Natn. Congr. Appl. Mech.*, 1954, pp. 517–520.

[3] W. FLÜGGE, *Stresses in Shells*. Springer (1962).
[4] D. DRUCKER, Some implications of work hardening and ideal plasticity. *Q. appl. Math.* 7, 411 (1950).
[5] D. DRUCKER, A more fundamental approach to plastic stress–strain relations. *Proc. 1st U.S. Natn. Congr. Appl. Mech.*, 1952, pp. 487–491.
[6] R. VON MISES, Mechanik der plastischen Formänderung von Kristallen. *Z. angew. Math. Mech.* **8**, 161 (1928).
[7] J. C. GERDEEN, Shell plasticity—piecewise smooth trajectories on the Nakamura yield surface. Ph.D. Dissertation, Stanford University (1965).

(*Received* 30 *September* 1966)

Résumé—La flexion d'une plaque circulaire, simplement supportée sous deux charges normales uniformes de magnitudes différentes dans la région centrale et la couronne circulaire extérieure est considérée. Un matériel de plastique parfaitement rigide est assumé qui obéit à la condition de rendement de Tresca. Les solutions exactes sont déterminées en termes des moments, de flexion radiaux et circonférentiels. Un diagramme complet de charge de rupture à deux paramètres est construit, qui est régulier du côté de la pièce.

Une variété de mécanismes de rupture est exposée pour différents degrés de chargement. Particulièrement un mode de déflection à "deux façons" est découvert, la plaque peut dévier soit "en haut" soit "en bas" à certains degrés de charges opposantes. Un nouveau résultat de portée spéciale est démontré—des portions de quelques trajectoires de contrainte se trouvent dans le domaine rigide limité par la surface de rendement.

Zusammenfassung—Die Biegung einer einfach gestützten runden Platte unter zwei gleichförmigen Normallasten verschiedener Grösse, im Mittelbereich sowie im äusseren Ring, wird behandelt. Ein starres, vollkommen plastisches Material wird vorausgesetzt, das die Tresca'sche Fliessbedinung befolgt. Genaue Lösungen werden bestimmt und als Radial- und Ringbiegemomente ausgedrückt. Ein vollständiges Schaubild wird aufgebaut für die zweiparameter Zusammenbruchsbelastung, das Schaubild ist stückweise regelmässig. Verschiedene Zusammenbruchsmechanismen werden für die verschiedenen Belastungsverhältnisse gezeigt. Insbesondere wird eine "zweiweg" Durchbiegung gezeigt, wobei die Platten bei bestimmten Verhältnissen der gegenwirkenden Belastungen "auf" oder "ab" ausweichen können. Ein neues Resultat wird gezeigt, das von besonderer Wichtigkeit ist—Teile mancher Spannungstrajektorien liegen innerhalb der starren Domäne die von der Fliess-Oberfläche umgeben sind.

Абстракт—Рассматривается сгибание свободно опёртой круговой пластины под двумя однородными нормальными нагрузками различных размеров в центральной части и во внешнем круговом кольце. Предполагается совершенно твёрдый пластический материал, который удовлетворяет условию текучести Треска (Tresca yield). Определены точные решения с точки зрения радиальных изгибающих моментов окружности круга. Составлена полная диаграмма дву-параметрической критической нагрузки, которая кусочно правильна. Представлено многообразие разрушающих (критических) механизмов для различных соотношений нагрузок. В особенности найден "двусторонний" образ действия отклонения; пластина может отклоняться "вверх" или "вниз" при определённых соотношениях противопоставленных нагрузок.

Показан новый результат специального значения. Части некоторых траэкторий напряжения лежат в пределах твёрдой области, ограниченной поддающейся поверхностью.